DDT in Natural Gas-Air Mixtures on Large Scales: Experiments and Simulations

V. N. Gamezo[1], R. K. Zipf, Jr.[2], D. A. Kessler[1], E. S. Oran[1]

[1]*Laboratory for Computational Physics and Fluid Dynamics,*
Naval Research Laboratory, Washington, DC 20375

[2]*Office of Mine Safety and Health Research,*
National Institute for Occupational Safety and Health, Pittsburgh, PA 15236, USA

1 Introduction

Explosive mixtures of natural gas (NG) with air can create the environment for a large-scale disaster in any industry that deals with natural gas. The coal mining industry is particularly prone to accidental explosions because NG (mostly methane) is released by coal layers, and it is difficult to control in extensive, complex networks of underground tunnels. The potential explosion hazard is aggravated by the presence of combustible coal dust, and the multiple, often uncontrolled ways in which explosive mixtures can be ignited.

Though coal mine accidents in the USA have declined dramatically because of decades of research, new technology, and prevention programs [1], they continue to occur and result in a significant loss of life. Between 1976 and 2010, at least 25 explosions involving NG and coal dust occurred in the active areas of coal mines in the USA. From 1986 to 2006, at least 12 known explosions involving NG alone occurred in the abandoned and sealed areas of coal mines. A total of 185 coal miners were killed and many were seriously injured as a result of these explosions [2]. Many more explosions occur around the world, in particular in China, where fatalities in coal mine accidents are 40 times higher than in the USA [1].

Accidental explosions involving detonations are the most dangerous because they generate the highest pressures and can breach protective walls (seals) that separate active parts of coal mines from abandoned unventilated areas. Our abilities to predict the deflagration-to-detonation transition (DDT) in NG-air mixtures in coal mine environments are still very limited, mostly due to the lack of experimental data that could be used to validate numerical models for large scales characteristic of underground coal mines. Typical coal mine tunnels are about 2 m high, 6 m wide, and 500–5000 m long. Most of the DDT experiments for methane-air or NG-air mixtures that produced detonations were performed in tubes with diameters between 0.05 and 0.5 m and lengths up to 35 m [3–7]. A series of low-pressure DDT experiments were performed in a 61 cm diameter, 100 m long smooth tube [8]. Some preliminary data recently obtained in 1.05 m diameter, 73 m long tube at NIOSH also showed DDT [9]. An obstructed, 2.5 m diameter, 10 m long tube was used in experiments [10] that did not produce detonations but generated maximum pressures about 0.58 MPa. The largest NG-air explosion tests producing peak pressures above 3.2 MPa were carried out in a 57-m long experimental mine tunnel in Poland [11], but they are still small compared to realistic coal mine scales.

In this work, we report the results of DDT experiments for NG-air mixtures contained in a 1.05 m diameter, 73 m long tube at NIOSH Lake Lynn Laboratory. These results are used to extend the validation of numerical models that have been previously developed and validated on smaller scales for methane-air mixtures [12, 13].

2 Large-scale Experiments

Multiple large-scale tests on flame acceleration and DDT in NG-air mixtures were performed in 2012 by the NIOSH team using the Gas Explosion Test Facility (GETF). The facility, described in detail in [2,14], consists of a detonation tube closed at one end, diagnostic equipment, and supporting systems. The total length of the tube is 73 m, and the internal diameter d is 105 cm. For the DDT experiments, the tube was modified to include 15 obstructions (steel beams) placed perpendicular to the tube axis every 1.52 m starting at 2.3 m from the closed end of the tube. The obstructions blocked 0.13, 0.25, or 0.5 of the tube cross-sectional area, depending on the experiment. Natural gas concentration in test mixtures was varied between 5.1% and 15.0% by volume. Test mixtures were ignited with a commercially available electric match containing 0.45 g of pyrotechnic composition. The electric match was placed about 0.5 m from the closed end of the tube. The subsequent evolution of flames and pressure waves was recorded using 23 piezoelectric pressure transducers and 23 light sensors placed in pairs (pressure and light) every 3.1 m along the length of the tube.

Experimental results are summarized in Fig. 1 that shows flame velocities and maximum pressures measured at different locations for all tests. The ignition was achieved in NG-air mixtures containing between 6.1 and 14.1% NG. For this concentration range, the flame velocity at the end of the obstructed section of the tube increased to values above 300 m/s. Pressures above 1 MPa were measured in all tests over the composition range 6.5 to 12.4%. Fast sonic flames with velocities reaching the the sound speed in the combustion products (800 to 1000 m/s) were observed for mixtures containing 8.0-10.8% NG. Detonations were observed for the same range 8.0-10.8% NG. The normalized run-up length to sonic flame velocity X_S/d ranges from 17 to 23 at BR = 0.13, and 9 to 17 for BR = 0.25 and 0.50.

3 Numerical Model

Two-dimensional numerical simulations of flame acceleration and DDT for a model geometry similar to the experimental facility described in the previous section are presented below. We consider a rectangular channel, 4750 cm long and 104.4 cm wide, with solid obstructions placed uniformly along the lower and upper walls. The obstacles are 2 cm wide and 15.66 cm high, which corresponds to a blockage ratio of 0.3. The distance S between adjacent obstacles is equal to width of the channel, i.e., $S = d = 104.4$ cm. We assume the channel and flow field are symmetric about the centerline, and simulate only the bottom half. No-slip boundary conditions are applied at the left ($x = 0$) and bottom ($y = 0$) walls and along the surfaces of the rectangular obstructions. The right boundary is left open to the atmosphere, and zero-gradient outflow conditions are specified.

We consider a stationary stoichiometric NG-air gas mixture at 298 K that completely fills the channel. The mixture is ignited by a simulated spark on the channel centerline at the left end of the domain at $t = 0$. The total energy released from this small quarter-circular region (radius 0.25 cm) of burned material is approximately 100 mJ, and the weak shock created by the rapid energy conversion is not nearly strong enough to ignite a detonation directly. It does, however, perturb and distort the symmetric flame bubble and promote the growth of natural instabilities that are inherent in real systems.

The reactants are assumed to be fully premixed and behave as an ideal gas, so that the flow is governed by the compressible reactive Navier-Stokes equations coupled to the one-step Arrhenius kinetics of energy

release. The details of the chemical model are summarized in [12] including the full set of calibrated parameters (Table 1 in [12]).

The reactive Navier-Stokes equations are solved using an explicit, second-order, Godunov-type numerical scheme incorporating a Riemann solver and a structured adaptive mesh based on the fully-threaded tree algorithm [15]. The mesh refinement is dynamically controlled by gradients of density, pressure, and fuel mass fraction. Away from discontinuities, the maximum grid spacing is 0.29 cm, and in areas where the grid is refined, the minimum computational cell size, dx_{min}, is 0.0181 cm, which corresponds to approximately 3 computational cells per laminar flame thickness. Because dx_{min} is limited by the available computational resources, the simulations must be somewhat under-resolved. Thus, the computed laminar flame speed is slightly smaller than the theoretical laminar flame speed. These deviations are small ($< 10\%$) and are only of consequence near the very beginning of the simulations, before the growth in flame surface is dominated by flow instabilities. Kessler et al. [12] show that variation in S_l has little impact on the large-scale flame acceleration.

4   Numerical Results

Snapshots of the computed temperature field in the vicinity of the leading edge of the flame at several instants in time are shown in Fig. 2. The behavior of the flame brush is similar to that observed in smaller-scale systems [12].

After an initial expansion period, the flow field, induced by thermal expansion of the hot product gases, stretches the flame across several obstacles and causes the front to wrinkle (Fig. 2a). This stretching and wrinkling caused by Rayleigh-Taylor and Kelvin-Helmholz instabilities leads to an increase in total flame surface area and, accordingly, an increase in global energy release rate. The positive feedback between the acceleration of the induced flow field and the growth in total flame surface area leads to a rapidly expanding flame brush, whose leading edge moves quickly through the channel, leaving large pockets of unburned gas between obstacles for the trailing portions of the flame to consume (Fig. 2b). Eventually, the flame reaches the sound speed in the unburned mixture, and pressure pulses begin to pile up in front of the reaction zone (Fig. 2c). The flame brush continues to accelerate into this compressed unburned material as the total amount of flame surface continues to grow. The pressure pulses eventually coalesce into a strong leading shock (Fig. 2d). The resulting shock-flame complex continues to accelerate and its velocity approaches the sound speed in the burned gases, corresponding to roughly half of D_{CJ}. The diffraction of the leading shock over the obstacles causes Mach reflection in the space between adjacent obstructions. These Mach stems become stronger as the leading shock accelerates. When a strong Mach stem collides with the base of the next obstacle, the temperature is locally high enough to initiate reaction (Fig. 2e). Whether this reaction can trigger a detonation depends on the the local reactivity gradient in the hot spot. Figures 2f and 2g show the expansion of the reaction wave emanating from the hot spot through the space between the obstacle and leading edge of the reaction zone. Here, conditions were right for a detonation to form and then propagate through the remainder of the channel (Fig. 2h).

Figures 3a and 3b show the position of the leading edge of the flame brush as a function of time and the velocity of the flame brush as a function of the position of its leading edge, respectively. Both figures show the rapid acceleration of the flame front and the DDT event that occurs near 17 m, corresponding to the ignition event shown in Figs. 2e–g. The abrupt change in slope of the $x-t$ curve in Fig. 3a indicates the transition between the slower deflagration and faster detonation. The velocity of the propagating detonation quickly decays to a near steady speed of approximately 1875 m/s (Fig. 3b), which is close to D_{CJ} for this mixture.

3

5 Discussion and Conclusions

The run-up distance to DDT, L_{DDT}, computed for BR=0.3 is about 17 m, and it is consistent with the results of GETF experiments for BR=0.25. These large-scale results combined with earlier experiments [5] in smaller channels and plotted in Fig. 4 show that the L_{DDT}/d ratio decreases for larger channels. The results are valid for BR=0.3 and can be roughly extrapolated to larger scales either in the $log(d) - L_{DDT}/d$ or the $log(d) - L_{DDT}$ planes. For the typical size of coal mine tunnels, $d = 3$ m, these extrapolations give $L_{DDT} = 18$ and 27 m, respectively.

Since typical lengths of coal-mine tunnels greatly exceed the estimated L_{DDT}, it is very likely that detonation can develop during accidental NG-air explosions in coal mines. Even without detonations, the maximum pressures measured in GETF experiments for the composition range 6.5-12.4% NG exceed the limit of 0.8 MPa required for protective seals by coal mine safety regulations in the U.S.

References

[1] Mining Disasters. New York Times, Dec. 6, 2011. http://topics.nytimes.com/top/reference/timestopics/subjects/m/mines_and_mining/mining_disasters/index.html

[2] R.K. Zipf, Jr., V.N. Gamezo, M.J. Sapko, W.P. Marchewka, K.M. Mohamed, E.S. Oran, D.A. Kessler, E.S. Weiss, J.D. Addis, F.A. Karnack, D.D. Sellers. Journal of Loss Prevention in the Process Industries. (in press). Available online 27 May 2011. http://www.sciencedirect.com/science/article/pii/S0950423011000581

[3] W. Bartknecht, Explosion. Berlin, Germany: Springer-Verlag; 1981.

[4] R.P. Lindstedt, H.J. Michels. *Combust. Flame* 76 (1989) 169–181.

[5] M. Kuznetsov, G. Ciccarelli, S. Dorofeev, V. Alekseev, Yu. Yankin, T.H. Kim. *Shock Waves* 12 (2002) 215–220.

[6] M. Kuznetsov, M. Liberman, and I. Matsukov. *Combust. Sci. Technol.* 182 (2010) 1628–1644.

[7] M. Kuznetsov, V. Alekseev, I. Matsukov, T.H. Kim. Ignition, Flame Acceleration and Detonations of Methane-Air Mixtures at Different Pressures and Temperatures. Proceedings of 8th International Symposium on Hazards, Prevention, and Mitigation of Industrial Explosions, Yokohama, Japan, September 5-10, 2010, paper ISH-118.

[8] M. Gerstein, E.D. Carlson, F.U. Hill. *Industrial and Engineering Chemistry* 46 (1954) 2558–2562.

[9] R.K. Zipf, Jr., V.N. Gamezo, M.J. Sapko, W.P. Marchewka, K.M. Mohamed, E.S. Oran, D.A. Kessler, E.S. Weiss, J.D. Addis, F.A. Karnack, D.D. Sellers. Preliminary Large-scale DDT Experiments at NIOSH Lake Lynn Laboratory. Proceedings of 23rd ICDERS, Irvine, California, 2011.

[10] B. H. Hjertager, K. Fuhre, M. Bjorkhaug. *Combust. Sci. Technol.*, 62 (1988) 239–256.

[11] R.K. Zipf, Jr., M.J. Sapko, J.F. Brune. Explosion Pressure Design Criteria for New Seals in U.S. Coal Mines. NIOSH Publication No. 2007-144, Information Circular 9500, 2007 July; :1-76. http://www.cdc.gov/niosh/mining/pubs/pdfs/2007-144.pdf

[12] D.A. Kessler, V.N. Gamezo, E.S. Oran. *Combust. Flame* 157 (2010) 2063–2077.

[13] E.S. Oran, V.N. Gamezo, D.A. Kessler. Deflagrations, Detonations, and the Deflagration-to-Detonation Transition in Methane-Air Mixtures. NRL Memorandum Report 6400–11-9332, 2011. http://lcp.nrl.navy.mil/publications/NIOSH-DDT-NRL-6400–11-9332.pdf

[14] V.N. Gamezo, R.K. Zipf, Jr., M.J. Sapko, W.P. Marchewka, K.M. Mohamed, E.S. Oran, D.A. Kessler, E.S. Weiss, J.D. Addis, F.A. Karnack, D.D. Sellers. *Combust. Flame*, 159 (2012) 870-881.

[15] A.M. Khokhlov. *J. Comput. Phys.* 143 (1998) 519–543.
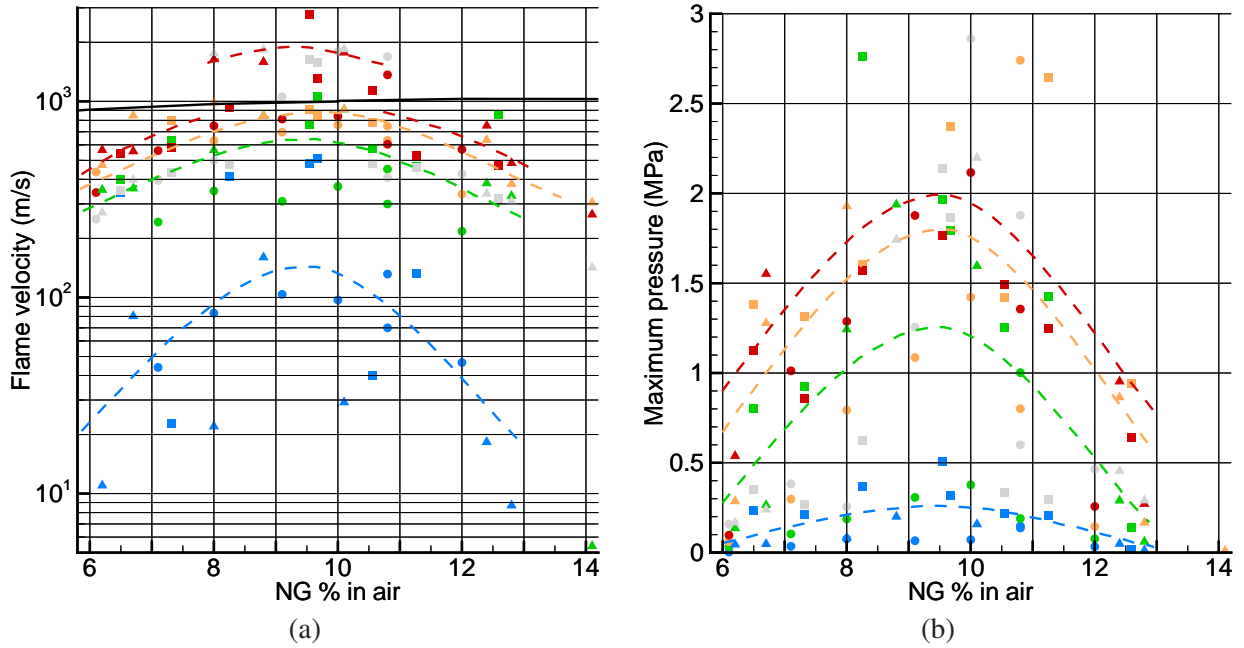
Figure 1: Flame velocity (a) and maximum pressure (b) measured at different locations for all tests: **blue** - at 5.94 m after 3 baffles, **green** - at 12.04 m after 7 baffles, **orange** at 18.14 m after 11 baffles, **red** - at 24.23 m after 15 baffles, **gray** - at 73.03 m (exiting tube). Each dashed line approximately averages all measurements at one location. Black solid line shows sonic velocity in burned gas. BR = 0.13 (**circles**), 0.25 (**triangles**), 0.50 (**squares**).
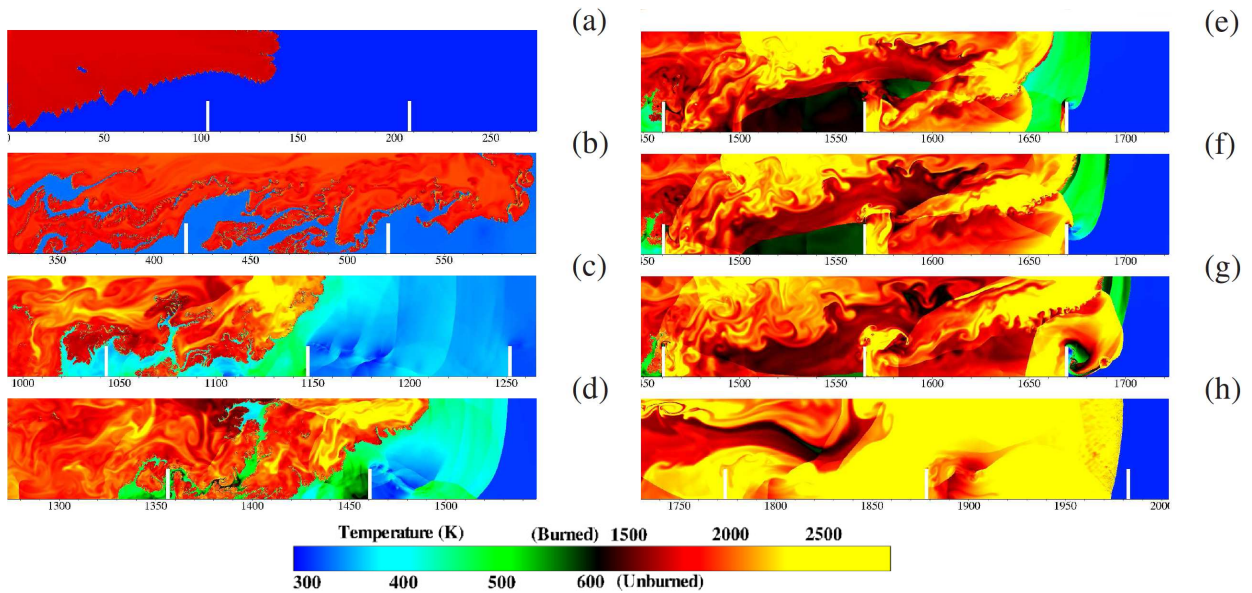
Figure 2: Temperature field near the leading edge of the reaction zone at $t =$ (a) 132.7 ms, (b) 191.6 ms, (c) 204.8 ms, (d) 209.1 ms, (e) 211.0 ms, (f) 211.06 ms, (g) 211.17 ms, and (h) 212.5 ms after spark ignition.

(a)

(b)
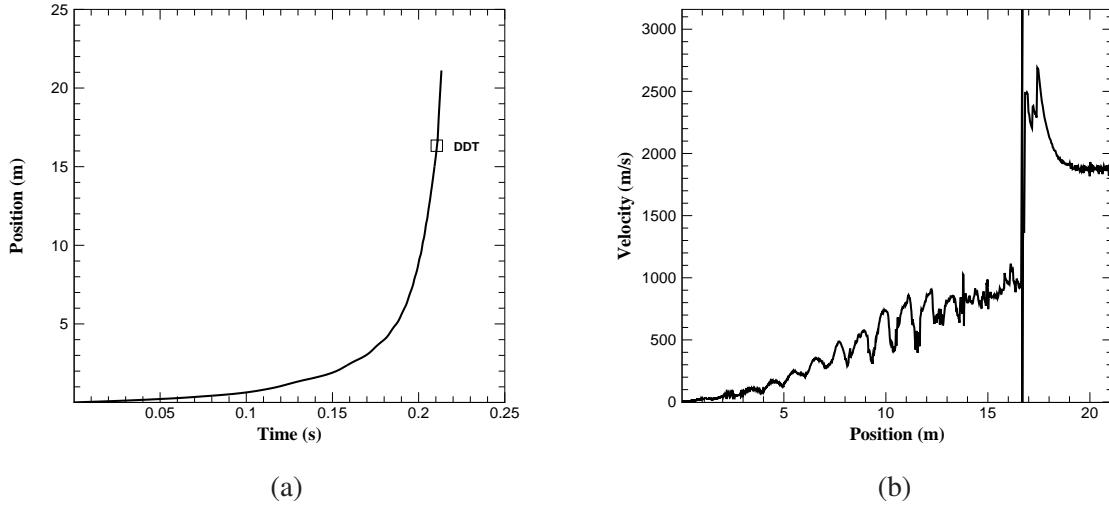
Figure 3: (a) Position of the leading edge of the reaction zone as a function of time and (b) velocity of the reaction zone as a function of its position in the channel for the case shown in Figure 2

(a)

(b)
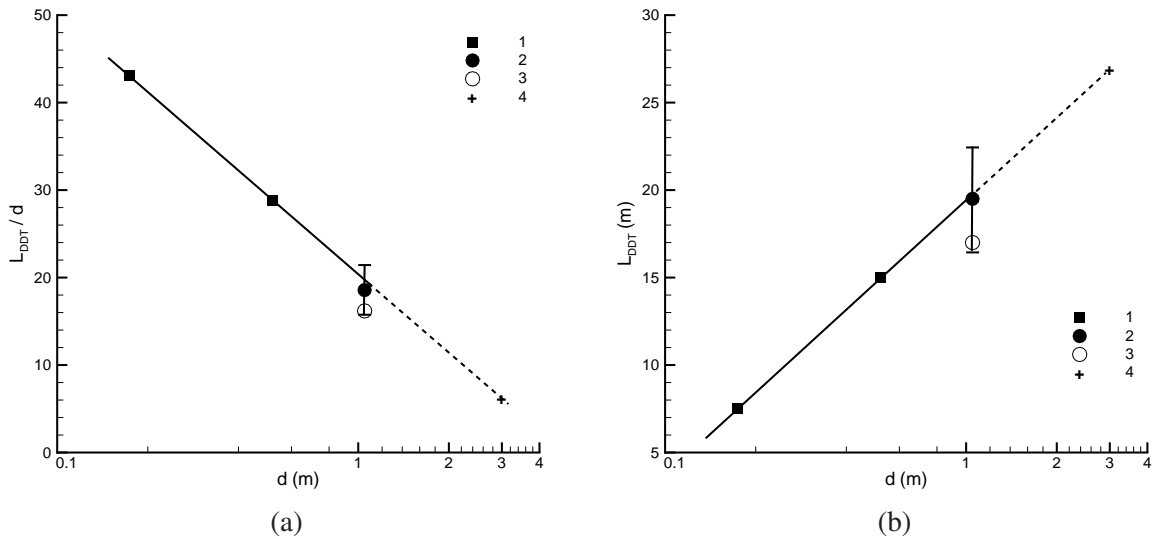
Figure 4: Run-up distance to DDT L_{DDT} in obstructed tubes and L_{DDT}/d ratio as functions of tube diameter d measured or computed for the stoichiometric methane-air mixture at 1 atm. 1 - experiment [5], BR=0.3, S=d=17.4 and 52 cm; 2 - GETF experiments, BR=0.25, d=1.05 m, S=1.52 m; 3 - calculation, BR=0.3, S=d=1.044 m; 4 - extrapolation to d = 3 m